Available online at www.CivileJournal.org

Civil Engineering Journal

(E-ISSN: 2476-3055; ISSN: 2676-6957)

Vol. 12, No. 04, April, 2026

Decoupling Chemical Composition from Viscoelastic Recovery in Rejuvenated Asphalt Binders

Multazam Hutabarat [1], Suwaphit Chamwon [1], Preeda Chaturabong [1*]

[1] *School of Engineering, King Mongkut's Institute of Technology Ladkrabang, Bangkok 10520, Thailand.*

Received 10 January 2026; Revised 21 March 2026; Accepted 28 March 2026; Published 01 April 2026

Abstract

This study investigates the decoupling between bulk chemical composition and high-temperature viscoelastic recovery in rejuvenated asphalt binders. A pressurized aging vessel (PAV)-aged binder (AC60/70) was rejuvenated using pyrolytic bio-oils from sugarcane bagasse (SBO) and rice straw (RSO) at 5–20 wt% dosages. SARA fractionation, colloidal instability index (Ic), penetration, and multiple stress creep recovery (MSCR) testing at 0.1 and 3.2 kPa were conducted before and after a rolling thin film oven (RTFO) aging. Both bio-oils restored SARA fractions to nearly identical levels (Ic = 0.541–0.572), yet penetration diverged substantially (79 vs. 36 dmm at 20% for SBO and RSO, respectively). After RTFO aging, MSCR responses converged across all formulations regardless of pre-aging differences, yielding identical an Equivalent Single Axle Load (ESAL) classification. This convergence is attributed to selective volatilization of low-molecular-weight bio-oil components during thermal conditioning, consistent with findings from a companion rheological–fatigue study. The results reveal a fundamental decoupling: bulk chemical indices, while useful for compositional assessment, do not correspond to stress-dependent viscoelastic recovery mechanisms governing rutting resistance. Performance-based rheological testing is therefore essential for reliable evaluation of rejuvenated binders under field-relevant conditions.

Keywords: Bio-Oil Rejuvenation; SARA Fractionation; MSCR Test; Colloidal Instability Index; Asphalt Aging; Sugarcane Bagasse Oil; Rice Straw Oil.

1. Introduction

Asphalt binder constitutes the fundamental binding matrix in flexible pavements, providing critical performance attributes including mechanical stability, constructability, acoustic dampening, and maintenance efficiency [1]. The inherent recyclability of asphalt materials has positioned reclaimed asphalt pavement (RAP) as a strategic component of sustainable infrastructure development. Large-scale RAP incorporation yields substantial environmental dividends—reducing virgin material consumption and lowering greenhouse gas emissions—while simultaneously delivering economic benefits through decreased material procurement costs. However, the oxidative aging processes occurring throughout pavement service life fundamentally alter RAP binder chemistry and performance characteristics. These aging manifests as progressive depletion of light maltene fractions, particularly aromatic compounds, concurrent with accumulation of polar resins and high-molecular-weight asphaltenes [2]. These compositional shifts induce profound property changes: increased elastic modulus, reduced phase angle, diminished ductility, and compromised resistance to fatigue cracking under traffic loading [3].

The deterioration of high-temperature rutting resistance represents a particularly complex consequence of asphalt aging. While oxidative stiffening initially appears beneficial for permanent deformation resistance, the concurrent loss

* Corresponding author: preeda.ch@kmitl.ac.th

https://doi.org/10.28991/CEJ-2026-012-04-09

of viscoelastic recovery capacity creates critical vulnerabilities. Aged binders develop brittle microstructures prone to microcrack nucleation under repeated loading cycles, which subsequently propagate to form macroscopic rutting damage [4]. This dichotomy—enhanced stiffness coupled with reduced elastic recovery—necessitates strategic rejuvenation approaches that restore balanced rheological properties. Effective rejuvenators must simultaneously reduce viscosity to improve workability, restore maltene-to-asphaltene ratios to enhance ductility, and maintain sufficient elastic recovery to resist permanent deformation under cyclic loading conditions [5].

Bio-oils derived from lignocellulosic biomass via fast pyrolysis have demonstrated substantial promise as renewable asphalt rejuvenators [6, 7]. These thermochemical conversion products contain abundant oxygenated functional groups including phenolic hydroxyl, carbonyl, carboxyl, and ester moieties that facilitate interactions with aged asphalt components through multiple mechanisms [8–10]. Despite extensive investigation of bio-oil rejuvenators derived from diverse feedstocks—including wood residues, vegetable oils, and agricultural wastes—systematic comparative studies of chemically distinct agricultural biomasses remain limited. Most existing research has focused on empirical performance evaluation without establishing fundamental relationships between bio-oil molecular composition, bulk chemical indicators, and stress-dependent mechanical behavior [11]. Hutabarat et al. [12] demonstrated through integrated chemical, rheological, and fatigue evaluation that chemical indices alone cannot fully describe rejuvenation effectiveness or aging progression, and that performance benefits are substantially diminished after secondary aging regardless of bio-oil type or dosage.

Bulk chemical characterization methods, particularly saturates–aromatics–resins–asphaltenes (SARA) fractionation and related indices such as the colloidal instability index (Ic), have been widely used to interpret the rheological behavior of asphalt binders. Numerous studies have reported correlations between SARA fractions and conventional rheological indicators, suggesting that increases in asphaltenes and resins generally enhance stiffness and deformation resistance, while higher saturates and aromatics contents are associated with improved flowability and relaxation behavior [13]. As a result, these bulk chemical indices are frequently employed to infer the effectiveness of aging, modification, and rejuvenation processes. Despite their widespread use, SARA fractions and bulk chemical indices represent averaged compositional information and do not explicitly account for loading mode, stress dependency, or delayed elastic response. Rheological parameters derived from cyclic creep and recovery, such as those obtained from the multiple stress creep recovery (MSCR) test—which measures percent recovery (%R) and non-recoverable creep compliance (Jnr)—capture viscoelastic recovery mechanisms that are fundamentally different from stiffness- or viscosity-based indicators [14]. Consequently, whether changes in bulk chemical indices can reliably explain high-temperature viscoelastic recovery, particularly after aging, remains insufficiently understood for rejuvenated systems containing complex polar and volatile constituents.

This uncertainty is especially relevant because chemical restoration does not necessarily imply mechanical recovery. Previous studies have shown that rejuvenators can substantially alter SARA distributions and penetration-related properties, while their effects on stress-dependent recovery behavior may diminish after short-term aging or under higher stress levels [7, 15]. Indeed, the companion study by Hutabarat et al. [12] on the same bio-oil systems confirmed that fresh rejuvenation benefits are largely eliminated after RTFO–PAV aging, with only minimal-dosage formulations (5% SBO) retaining statistically significant protection. Such observations suggest that apparent chemical rebalancing may not translate directly into sustained viscoelastic recovery under high-temperature cyclic loading conditions.

Unlike previous studies that have examined chemical and rheological properties independently, this investigation systematically demonstrates the decoupling between bulk chemical restoration and stress-dependent viscoelastic recovery in rejuvenated systems. It is hypothesized that bulk chemical composition is fundamentally decoupled from high-temperature viscoelastic recovery behavior in rejuvenated asphalt binders after aging, as measured by stress-dependent MSCR parameters. Accordingly, this study aims to (i) examine the relationship between bulk chemical indices and MSCR-derived recovery parameters in rejuvenated binders, (ii) evaluate the stability of these relationships after short-term aging, and (iii) characterize the extent of decoupling between chemical-based indicators and high-temperature viscoelastic recovery behavior. This work complements the authors' companion study [12], which addressed fatigue-based (LAS) performance, by focusing specifically on high-temperature rutting resistance through MSCR evaluation.

2. Materials and Methods

2.1. Materials

The base asphalt binder used in this study was AC60/70 grade, obtained from Tipco Asphalt Public Company Limited, Bangkok, Thailand, conforming to Thai Industrial Standard TIS 394. The physicochemical properties of the base binder are presented in Table 1. Two agricultural biomass feedstocks were selected for bio-oil production: sugarcane bagasse and rice straw, sourced from local farmers in the central region of Thailand.

Table 1. Physicochemical Properties of Base Asphalt Binder (AC60/70)

Property	Test Method	Unit	Value
Penetration at 25°C	ASTM D5	dmm	62
Softening Point	ASTM D36	°C	52
Ductility at 25°C	ASTM D113	cm	>100
Viscosity at 135°C	ASTM D4402	Pa·s	0.38
Viscosity at 165°C	ASTM D4402	Pa·s	0.17
Specific Gravity	ASTM D70	—	1.03
Flash Point	ASTM D92	°C	> 230
Solubility in TCE	ASTM D2042	%	> 99.5

2.2. Aging Simulation

The laboratory aging simulation was conducted under two conditions: short-term aging using a Rolling Thin Film Oven (RTFO) following ASTM D2872, and long-term aging using a Pressurized Aging Vessel (PAV) following ASTM D6521 [16, 17]. For RTFO conditioning, 35 g of heated asphalt binder was poured into glass bottles and placed on the rotating carriage. Samples were conditioned for 85 minutes at 163°C with an airflow rate of 4000 mL/min, simulating short-term aging during mixing and paving operations. Afterwards, the RTFO-aged binders were subjected to PAV conditioning for long-term aging simulation, representing approximately 5 years of in-service oxidative aging. Fifty grams of RTFO-aged binder was poured into plates and placed vertically in the PAV rack, then exposed for 20 hours at 90–100°C under a pressure of 2.07 MPa (300 psi). In this research, PAV-aged asphalt binder is considered to have properties comparable to aged RAP binder recovered from the field [18].

2.3. Pyrolysis and Distillation

The pyrolysis process began with drying the biomass feedstocks to reduce moisture content. The dried biomasses were subjected to pyrolysis in a fixed-bed reactor under an inert nitrogen atmosphere to suppress oxidative reactions. The biomasses were rapidly heated to 500°C under fast-pyrolysis conditions, with short vapor residence times (<2 s) before rapid quenching to maximize liquid bio-oil recovery [12]. The resulting liquid products are hereafter referred to as SBO (Sugarcane Bagasse Oil) and RSO (Rice Straw Oil) [19-21], as illustrated in Figure 1.

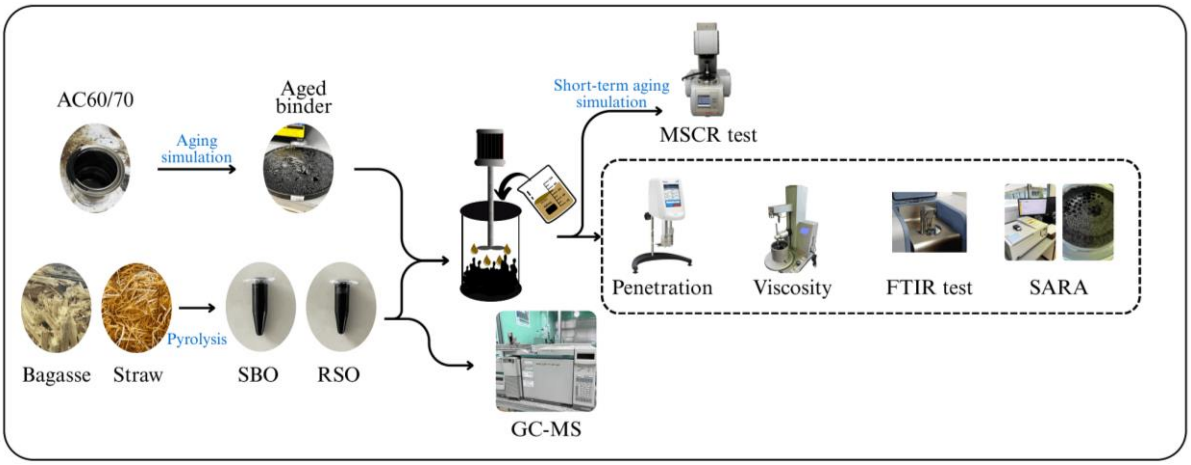

Figure 1. The Process of Rejuvenated Binders by Pyrolytic Oils

The pyrolysis temperature of 500°C was selected based on optimization for maximum liquid bio-oil yield under fast pyrolysis conditions, as detailed in the authors' companion study [12]. This temperature falls within the typical fast pyrolysis range (400–550°C) recognized for producing bio-oils with balanced aromatic content and adequate liquid recovery (typically 50–65% yield) [21, 22]. The resulting bio-oils contained substantial phenolic content (SBO: 42.84%; RSO: 40.67%) with distinct chemical profiles—SBO enriched in methoxy-phenolics and aromatic hydrocarbons, RSO dominated by catechol derivatives, nitrogenous species, and oxygenated sugar compounds [12, 22].

It should be noted that the composition of lignocellulosic biomass varies with cultivar, growing conditions, harvest timing, and post-harvest processing. Sugarcane bagasse typically contains 40–50% cellulose, 25–35% hemicellulose, and 15–25% lignin, while rice straw contains 30–45% cellulose, 20–30% hemicellulose, and 10–20% lignin [11, 22, 23]. This compositional variability may influence the chemical profile of the resulting bio-oil and should be considered when extending these findings to feedstocks from different geographic origins. The complete experimental workflow is summarized in Figure 2.

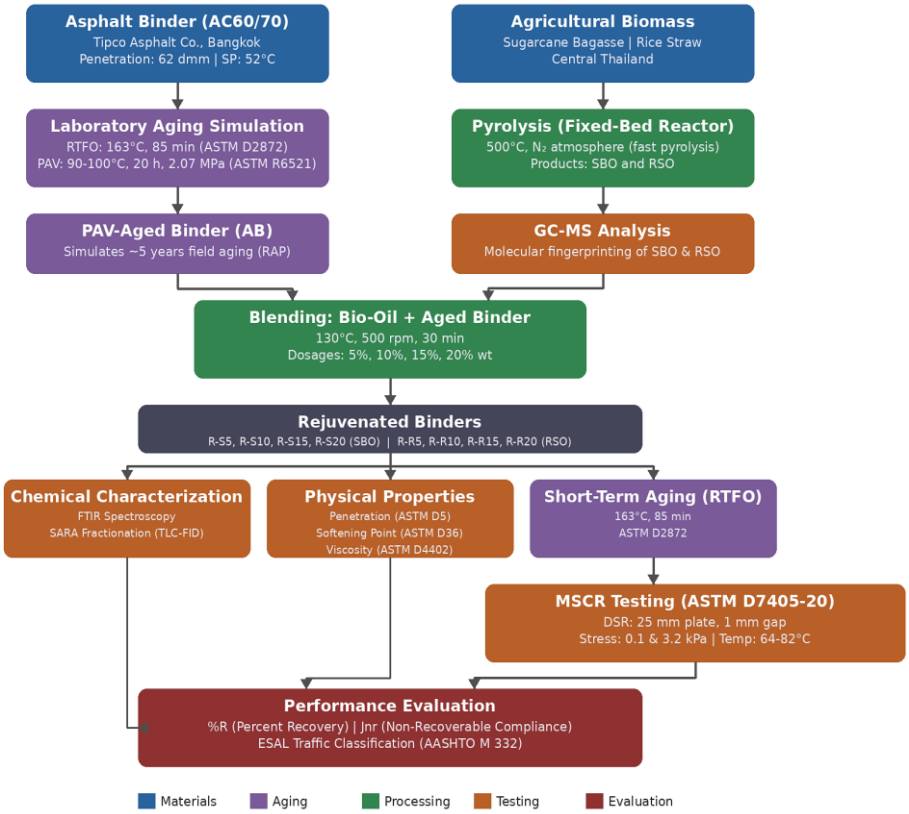

Figure 2. Experimental Methodology Flowchart

2.4. Gas Chromatograph–Mass Spectrometry (GC-MS) Test

The chemical composition of the pyrolytic bio-oils was analyzed using GC-MS [24]. It should be noted that GC-MS preferentially resolves thermally stable and volatile compounds while under-representing non-volatile or thermally labile constituents [25]. Complementary techniques such as gel permeation chromatography (GPC) and nuclear magnetic resonance (NMR) spectroscopy are recommended for future investigations. The GC analysis was performed on a capillary column (HP-5MS, 30 m × 0.25 mm ID, 0.25 µm film thickness) with helium as the carrier gas at a flow rate of 1.0 mL/min. Samples (1.0 µL) were injected in splitless mode, and the oven temperature was programmed from 40°C (held for 2 min) to 280°C at 10°C/min, with a final hold for 10 min. Ionization was carried out using electron impact (EI) at 70 eV, scanning m/z 40–550. Compound identification was achieved by comparing mass spectra with the NIST spectral library.

2.5. Mixing Process

Bio-oils were incorporated into the PAV-aged asphalt binder at concentrations of 5%, 10%, 15%, and 20% by weight (wt%). A high-shear mixer operating at 500 rpm for 30 minutes at a constant temperature of 130°C was used to ensure homogeneous blending. The mixing temperature of 130°C was selected to exceed the softening point of the aged binder (~68°C) while remaining below the RTFO conditioning temperature (163°C) to minimize additional oxidative aging during preparation. Preliminary viscosity measurements confirmed adequate homogenization [26, 27].

The dosage range of 5–20 wt% was selected based on published literature [6, 7, 26, 27] and preliminary penetration screening, which indicated that dosages below 5% produced negligible softening while dosages above 20% resulted in excessive softening exceeding specification limits. Field applications typically use 8–15% depending on RAP content and target grade.

The asphalt binders are denoted as follows: Base for the neat binder; R-Base for the short-term aged binder; and AB for the sequentially short-term and long-term aged binder. The rejuvenated binders are designated based on their bio-oil type and dosage: R-R5 through R-R20 for rice straw oil, and R-S5 through R-S20 for sugarcane bagasse oil [26].

2.6. Fourier Transform Infrared (FTIR) Test

Functional group analysis of the asphalt binders was conducted using FTIR spectroscopy, which identifies molecular functional groups based on their characteristic vibrational frequencies (wavenumber, cm^{-1}) and absorption intensities.

The test was conducted using a PerkinElmer Spectrum 10.5.0 spectrometer in attenuated total reflectance (ATR) mode, which is insensitive to sample shape and color. One gram of solid asphalt binder was prepared for each measurement. All specimens were scanned 16 times over a wavenumber range from 400 to 4000 cm^{-1} [28].

2.7. Saturates, Aromatics, Resins, Asphaltenes (SARA) Fractionation

One gram of asphalt binder was dissolved in 30 mL of n-heptane, followed by ultrasonic treatment for 10 minutes and partially immersed in a 50°C water bath for 15 minutes to ensure thorough dispersion. The sample was then cooled at 18°C for 45 minutes to precipitate asphaltenes. Filtration was conducted to separate the maltene fraction from the asphaltene precipitate. An aliquot of 1 µL of the maltene was applied to chromarods and analyzed using thin-layer chromatography with flame ionization detection (TLC-FID). This method quantified the sub-fractions of maltene—namely saturates, aromatics, and resins—based on peak areas recorded. The colloidal instability index (Ic) was calculated to assess the stability of the asphalt binder's colloidal structure using Equation 1, as formulated by Zhou et al. [29].

$$I_c = \frac{\%Saturates+\%Asphaltenes}{\%Aromatics+\%Resins} \quad (1)$$

2.8. Physical Properties (Penetration and Viscosity)

Penetration was measured at 25°C in accordance with ASTM D5, quantifying the depth (in decimillimeters, dmm) to which a standard needle penetrates the binder surface under a 100 g load over 5 seconds. Softening point was determined by the ring-and-ball method, indicating the temperature at which asphalt binder softens under a standardized load following ASTM D36. Viscosity was measured at 135°C and 165°C using a Brookfield rotational viscometer in accordance with ASTM D4402, quantifying the binder's resistance to flow under shear [30, 31].

2.9. Multiple Stress Creep Recovery (MSCR) Test

The MSCR test was performed using a dynamic shear rheometer (DSR) equipped with 25 mm parallel plate geometry and a 1 mm testing gap, following the standardized procedure outlined in ASTM D7405-20. RTFO-aged asphalt binders were subjected to 10 loading cycles at each stress level: 0.1 kPa and 3.2 kPa, at temperatures of 64–82°C [14]. Each cycle comprised a 1-second loading phase followed by a 9-second recovery period, during which the strain response was continuously recorded (Figure 3). The deformation behavior during each cycle was characterized by two parameters: percent recovery (%R), representing the recoverable (elastic) deformation, and non-recoverable creep compliance (Jnr), representing permanent deformation susceptibility, calculated using Equations 2 and 3, where ε_r is the recovered strain, ε_nr is the non-recovered strain, ε_0 is the initial strain at peak load, and σ_0 is the applied stress [1, 14].

$$\%\ R = \frac{\varepsilon_r}{\varepsilon_0} \times 100 \quad (2)$$

$$J_{nr} = \frac{\varepsilon_{nr}}{\sigma_0} \quad (3)$$

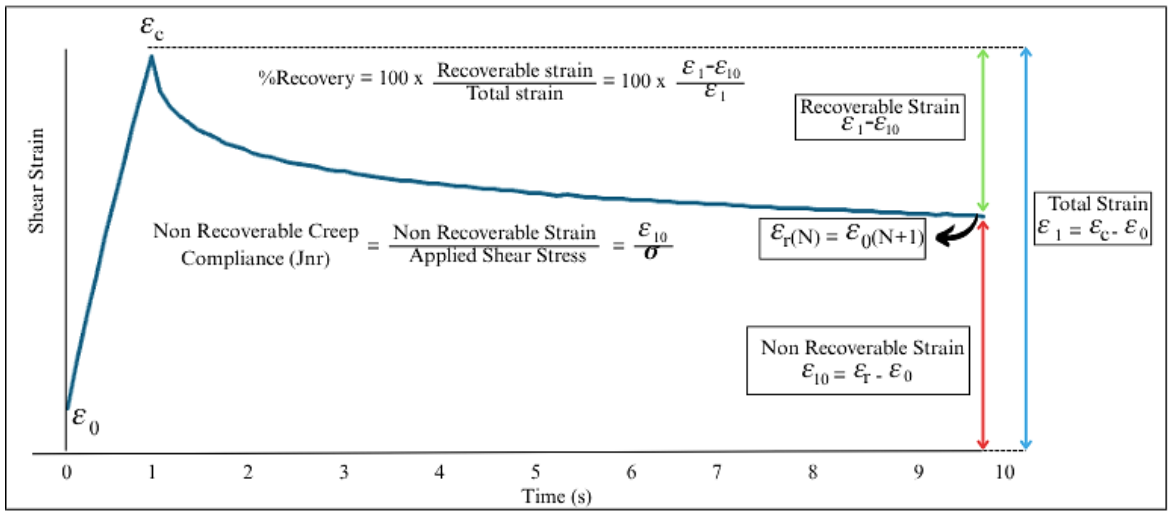

Figure 3. Creep and Recovery in Individual Cycle of MSCR

3. Results and Discussion

3.1. Molecular Architecture and Rejuvenation Mechanisms: GC-MS Characterization

The molecular composition of pyrolytic bio-oils fundamentally dictates their capacity to restore aged asphalt through specific chemical interactions at the colloidal scale. GC-MS analysis identified 45 and 25 distinct compounds in SBO and RSO, respectively (Tables 2 and 3), with retention times predominantly below 20 minutes—a temporal signature consistent with volatile, low-molecular-weight species. This detection pattern reflects the inherent limitation of GC-MS methodology, which preferentially resolves thermally stable and volatile compounds while under-representing non-volatile or thermally labile constituents [25]. As noted in Section 2.4, complementary techniques including GPC and NMR spectroscopy would provide a more comprehensive molecular characterization.

Table 2. Chemical Characterization of Sugarcane Bagasse Oil (SBO)

Chemical Class	Representative Compounds	Total (%wt)	All compounds
Phenolic Compounds	Phenol, Cresols, Guaiacol, Syringol, Xylenols	42.84	p-Ethylphenol; Syringol; p-Cresol; Phenol; o-Cresol; 2,4-Xylenol; Guaiacol; Catechol; 3-Methylcatechol; 2-Ethyl-5-methylphenol; 6-Methylguaiacol; 4-Methylcatechol; 2,3-Xylenol; p-Propylguaiacol; Hydroquinone; E-Isoeugenol; 2,5-Xylenol; Eugenol methyl ether
Methoxy Aromatic	Dimethoxybenzene, Methoxy-substituted compounds	12.05	2,3,5-Trimethoxytoluene; Benzeneethanol, 2-methoxy; p-Dimethoxybenzene
Sesquiterpnes/Terpenes	β-Caryophyllene, Cyclic terpene structures	6.76	β-Caryophyllene; 1H-Cycloprop[e]azulene, decahydro-1,1,7-trimethyl-4-methylene; 1H-Cycloprop[e]azulene, decahydro-1,1,7-trimethyl-4-methylene; Ledene
Aromatic Hydrocarbons	Naphthalene, Methylnaphthalenes	8.75	Trimethylnaphthalene; Naphthalene; 2-Methylnaphthalene; 2-Methylnaphthalene; 2,3-Dimethylnaphthalene; 4-Octyne; 9H-Fluorene
Cyclic Ketones	Cyclopentenones, Furanones	6.07	2-Cyclopenten-1-one, 2-hydroxy-3-methyl; 2(3H)-Furanone, dihydro; Cycloocta-1,4-dien-3-one; 2-Cyclopenten-1-one, 3-methyl; 2-Cyclopenten-1-one, 3-ethyl-2-hydroxy
Furan Derivatives	Pyran derivatives	4.73	2H-Pyran-2,4(3H)-dione, 3-acetyl-6-methyl
Sugar Derivatives	Levoglucosan, Anhydroglucose	4.12	Anhydroglucose; Levoglucosan
Others	Miscellaneous compounds	14.68	2(3H)-Benzothiazolethione; Dimethylsilacyclobutane; Propoxur; 1,3-Butanediol; p-Ethylbenzaldehyde

Table 3. Chemical Characterization of Rice Straw Oil (RSO)

Chemical Class	Representative Compounds	Total (%wt)	All compounds
Phenolic Compounds	Phenol, Catechols, Syringol	40.67	Catechol; Syringol; 4-Methylcatechol; Hydroquinone; Phenol; 3-Methylcatechol
Nitrogen Compounds	Pyridones, Amines, Pyrazines	13.49	4-Pyridone; N-Methyl-1,3-propanediamine; 2,5-Dimethyl-3-propenylpyrazine; 6-Methyl-2-pyridone
Sugar Derivatives	Levoglucosan	13.21	Levoglucosan
Lactones/Furanones	Butyrolactones, Furan derivatives	12.33	γ-Butyrolactone; γ-Hydroxybutyrolactone; 3-Ethyl-2,5-dihydrofuran
Alcohols	Tetrahydrofurfuryl alcohol	11.37	Tetrahydrofurfuryl alcohol
Cyclic Ketones	Hydroxycyclopentenones	1.72	2-Hydroxy-3-methyl-2-cyclopenten-1-one
Carboxylic Acids	Vanillic acid	1.38	Vanillic acid
Others	Miscellaneous compounds	5.83	Various aliphatic, heterocyclic, and minor compounds

SBO's molecular fingerprint revealed a chemistry optimized for asphaltene solvation through aromatic compatibility mechanisms (Table 2). Phenolic derivatives—including phenol, cresols, guaiacol, and syringol—along with aromatic hydrocarbons constituted the dominant fraction [22]. These compounds function through dual mechanisms: their aromatic ring systems engage in π–π stacking interactions with the polyaromatic cores of aged asphaltenes, while phenolic hydroxyl groups provide hydrogen-bonding sites for polar sulfoxide and carboxylic acid functionalities introduced during oxidation. This molecular architecture facilitates effective solvation of asphaltene aggregates through aromatic compatibility. Beyond physical softening, phenolic hydroxyl groups are widely reported to act as sacrificial hydrogen donors capable of scavenging free radicals during thermal oxidation, which may contribute to improved aging resistance. Supporting molecular components—including cyclic ketones, furans, and terpenes—function as molecular spacers, infiltrating interstitial volumes between rigid asphalt chains and reducing intermolecular friction. Notably, sugar derivatives (levoglucosan, anhydroglucose) remained below 4%, minimizing potential incompatibility issues; elevated sugar content has been associated with poor solubility and moisture susceptibility [10].

RSO exhibited a contrasting molecular profile characterized by diminished aromatic solvent capacity and enrichment in polar heteroatomic species (Table 3). While phenolic compounds (catechol, syringol, hydroquinone) retained strong antioxidant functionality through free radical scavenging [32], the substantial nitrogenous fraction (13.49%)—comprising amines and pyridines—introduced polar functionalities that may enhance moisture resistance but compromise maltene resolvation. These nitrogen-containing heterocycles lack the nonpolar environment necessary for

complete peptization of asphaltene aggregates, thereby reducing fluxing capacity relative to aromatic solvents. The elevated sugar derivative content (13.21%) further compounds compatibility challenges; these rigid, hydrophilic oligosaccharides exhibit poor solubility in nonpolar asphalt matrices and may function as micro-fillers or form discrete stiff phases within the binder microstructure. Lactones and alcohols serve as amphiphilic bridging agents, mediating interfacial interactions between highly polar bio-oil components and the aromatic binder matrix [33].

The comparative molecular analysis indicates that the aromatic content of the rejuvenator plays a dominant role in rejuvenation efficacy. SBO's approximately 63% aromatic solvent fraction—comprising phenolics, methoxy aromatics, and aromatic hydrocarbons—ensures thermodynamic compatibility with aged asphaltene cores, enabling solvent-mediated peptization [34-37]. RSO, despite comparable antioxidant phenolic content (40.7%), is limited by enrichment in polar heteroatomic species that exhibit limited solubility in aromatic asphalt matrices. This fundamental chemical divergence establishes clear expectations: SBO should demonstrate superior softening efficacy and rheological recovery, while RSO's performance will be constrained by incompatible polar functionalities.

The GC-MS results are consistent with those reported in the authors' companion investigation [12], which confirmed that SBO is enriched with methoxy-phenolics and aromatic compounds while RSO contains higher proportions of catechol-type phenolics, nitrogenous species, and oxygenated sugars. Importantly, that study demonstrated that despite the high phenolic content (>40% for both bio-oils), these compounds provide primarily short-term rejuvenation through maltene replenishment and physical softening rather than sustained long-term antioxidant protection—a finding that further supports the present study's conclusion regarding the limitations of chemical indices as performance predictors.

3.2. Physical Property Restoration Through Molecular Diffusion Mechanisms

Penetration and softening point measurements quantify the macroscopic consequences of molecular-scale rejuvenation processes (Figure 4). Oxidative aging induced severe stiffening—penetration decreased from 62 dmm (Base) to 18 dmm (AB), while softening point increased from 52°C to 68°C—reflecting the thermodynamically driven collapse of asphalt molecular architecture under thermal and oxidative stress.

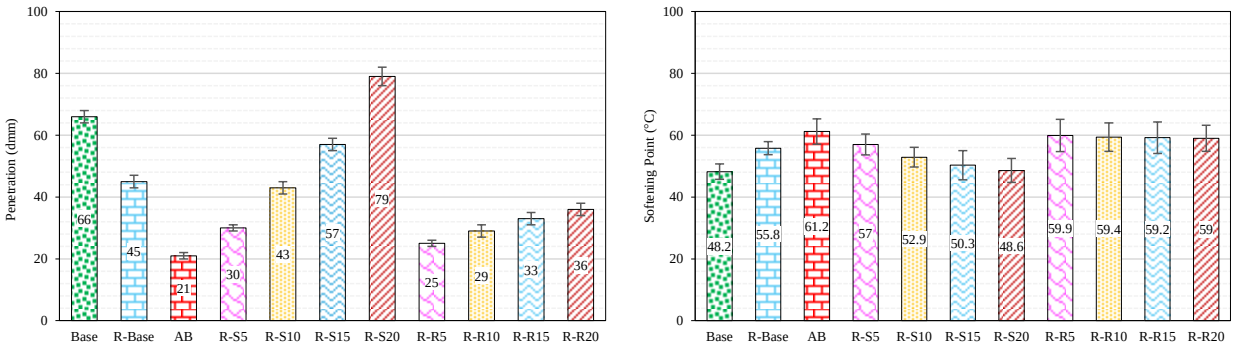

Figure 4. Penetration and Softening Points of Asphalt Binders

Bio-oil incorporation systematically reversed these aging-induced changes through diffusion-controlled fluxing mechanisms. Both SBO and RSO functioned as molecular lubricants, diffusing into interstitial voids within the aged binder matrix and disrupting asphaltene self-associations. However, the magnitude of restoration diverged dramatically. At 20% dosage, SBO restored penetration to 79 dmm—exceeding the virgin base binder—while RSO achieved only 36 dmm. This 119% performance differential reflects fundamental differences in chemical compatibility [27]. SBO's aromatic-rich composition provides solubility parameters closely matching aged asphaltene cores, enabling deep penetration and effective peptization. RSO's incompatible nitrogen and sugar functionalities provide only surface-level softening without fundamental microstructural reorganization.

These penetration recovery ratios are consistent with values reported in the literature. Waste cooking oil at 15–20% dosage has been reported to restore penetration to 60–80% of virgin binder values [29, 38-41], while vegetable oil-based rejuvenators achieved 70–90% recovery [27]. SBO at 20% exceeded 100% recovery, while RSO achieved only 58%, comparable to lower-efficiency waste oil rejuvenators [42].

Softening point data corroborate this interpretation. SBO treatment progressively decreased thermal transition temperatures (from 68°C at AB to 51°C at R-S20), indicating systematic disruption of asphaltene association networks. RSO produced more modest reductions. The dose-dependent restoration confirms that property recovery scales with the mass of introduced maltene-like components, though efficiency depends critically on molecular compatibility [41, 43].

The softening point reduction achieved by SBO (68°C → 51°C at 20% dosage, ΔSP = 17°C) is comparable to values reported by Wang et al. [42] for waste vegetable oil rejuvenation (ΔSP = 14–19°C at 15–25% dosage) and exceeds the 8–12°C reduction reported by Zargar et al. [37] for waste cooking oil at equivalent dosages. The more modest RSO softening (ΔSP = 9°C at 20%) aligns with the lower efficiency range reported for nitrogen-rich bio-based rejuvenators [6]. These comparisons confirm that aromatic-rich bio-oils consistently outperform polar-rich alternatives in thermal property restoration, independent of feedstock origin.

3.3. Viscosity-Temperature Relationships and Flow Activation Mechanisms

Rotational viscometry at 135°C and 165°C quantifies energy barriers governing molecular flow (Figure 5). Aging dramatically increased flow resistance—viscosity escalated from 0.38 Pa·s (Base) to 1.85 Pa·s (AB) at 135°C. Bio-oil incorporation functioned as viscosity modifiers through molecular dilution and lubrication. SBO demonstrated superior viscosity reduction capacity, achieving values approaching base binder levels across all dosages. RSO, while producing measurable reductions, consistently exhibited higher flow resistance at equivalent dosages [6, 42].

The viscosity-temperature susceptibility provides additional mechanistic insights. Aged binders exhibited viscosity ratios (η_{135} °C/η_{165} °C) of 3.2, indicating strong temperature dependence. SBO treatment normalized this ratio to 2.4–2.6, approaching the base binder value of 2.3, confirming effective dispersion of temperature-sensitive aggregates. RSO maintained elevated ratios (2.8–3.0), suggesting incomplete peptization. These results demonstrate SBO's superior fluxing efficiency across the entire temperature range relevant to asphalt processing [44].

The viscosity reduction efficiency of SBO (0.395–0.41 Pa·s at 135°C for 15–20% dosage) is consistent with findings by Zhang et al. [40], who reported viscosity reductions of 65–75% for wood-derived bio-oil at comparable dosages. Kumar & Aggarwal [6] reviewed that most bio-oil rejuvenators achieve 50–80% viscosity reduction at 10–20% dosage, within which SBO (76% reduction at 20%) falls at the upper range while RSO (58% reduction) occupies the mid-range. Notably, all rejuvenated formulations maintained viscosity below the Superpave mixing limit of 3.0 Pa·s at 135°C, confirming adequate workability for field applications.

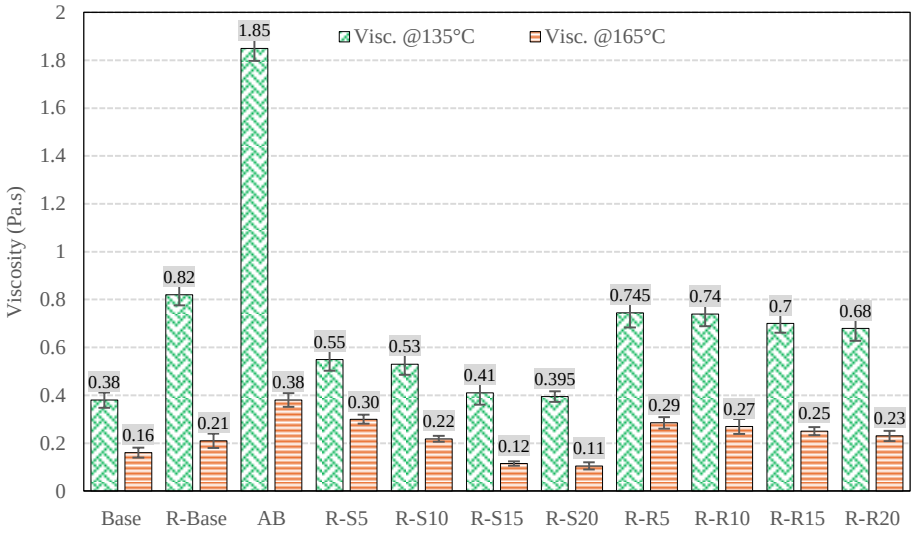

Figure 5. Viscosity of Asphalt Binders

3.4. Colloidal Rebalancing: SARA Fractionation

SARA fractionation quantifies colloidal restructuring achieved through bio-oil-mediated peptization (Figures 6 and 7, Table 4). Oxidative aging destabilized the colloidal system: the aromatic fraction decreased from 49.5% (Base) to 35.9% (AB), a 27% depletion, while asphaltenes doubled from 10.6% to 22.4%. This elevated the colloidal instability index from 0.272 to 0.508, approaching the transitional threshold (Ic > 0.7) beyond which gel-type behavior emerges [36].

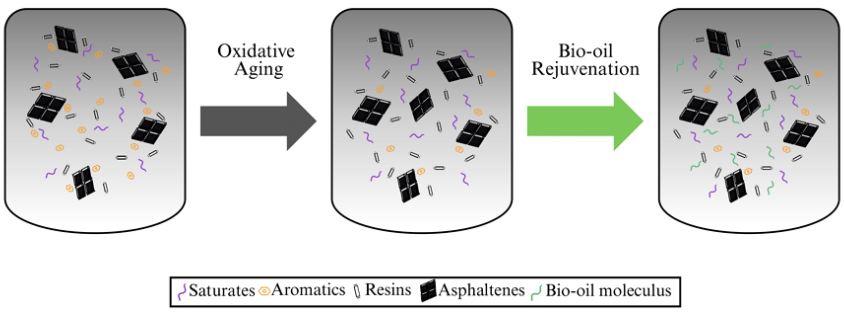

Figure 6. Aging and Rejuvenation Mechanism of Asphalt Binder

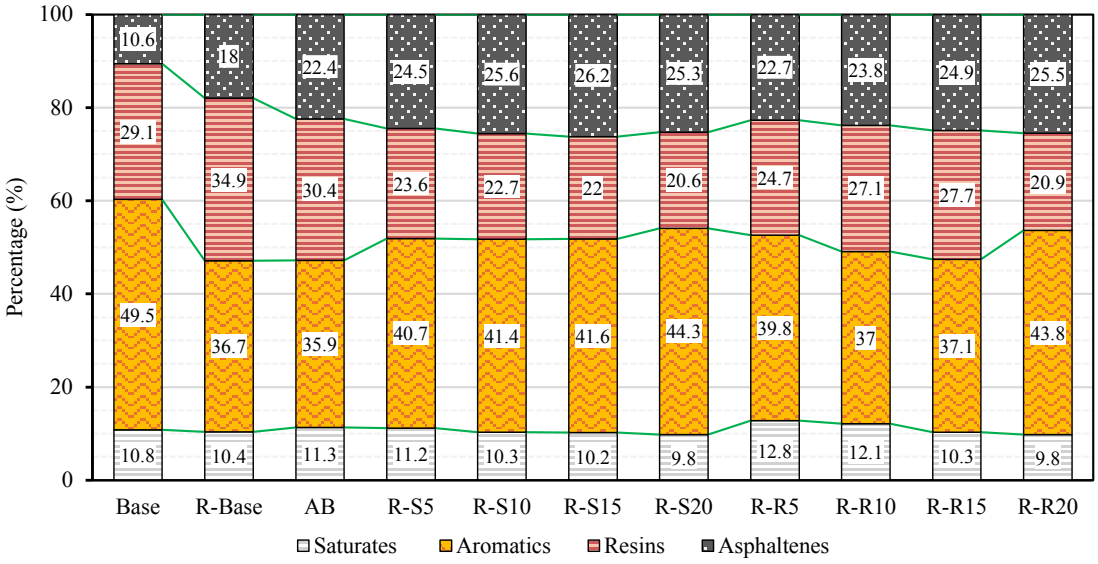

Figure 7. SARA Fractionations of Asphalt Binders

Table 4. The Colloidal Instability Index of Asphalt Binders

Sample	Base	R-Base	AB	R-S5	R-S10	R-S15	R-S20	R-R5	R-R10	R-R15	R-R20
Ic	0.272	0.397	0.508	0.555	0.560	0.572	0.541	0.550	0.560	0.543	0.546

Bio-oil rejuvenation systematically reversed this destabilization. At 20% dosage, SBO restored aromatics to 44.3%—recovering 62% of aging-induced depletion. However, the analytical asphaltene content remained elevated at 25.3%, which may partly reflect co-precipitation of polar bio-oil-derived compounds during n-heptane fractionation. The colloidal instability index decreased to 0.541, within the stable sol-type regime [7, 27].

Critically, RSO treatment produced comparable bulk SARA restoration, revealing a fundamental limitation: SARA fractionation captures only averaged compositional information. At 20% dosage, RSO restored aromatics to 43.8% with Ic = 0.546, matching SBO within experimental variability. This convergence contrasts sharply with the 119% penetration differential (79 vs. 36 dmm), providing direct evidence that SARA-derived indices have limited capacity to differentiate rejuvenator performance at the mechanical level.

The Ic values (0.541–0.572) align with literature benchmarks, where values below 0.7 indicate favorable sol-type characteristics, 0.7–1.2 represent transitional systems, and values exceeding 1.2 signify gel-type behavior [36, 37, 38]. This convergence directly demonstrates the decoupling identified in the hypothesis: chemical indices that correlate with penetration and viscosity do not extend to cyclic creep-recovery behavior.

This decoupling between SARA-derived indices and mechanical performance has not been widely reported in the rejuvenation literature. Most previous studies, including Xu et al. [13] and Wang et al. [38], reported positive correlations between SARA fractions and rheological indicators for unmodified binders. However, those correlations were established using conventional stiffness and viscosity parameters rather than stress-dependent recovery metrics. The present findings suggest that while SARA correlations may hold for equilibrium-type rheological properties (penetration, viscosity, |G*|), they break down for non-equilibrium, cyclic recovery behavior (MSCR %R, Jnr) where microstructural features—such as irreversible crosslinks and volatile-sensitive phases—dominate the response.

3.5. Spectroscopic Signatures of Molecular Interactions: FTIR Analysis

FTIR spectroscopy provides molecular-level evidence for aging-induced oxidation and bio-oil-mediated restoration (Figures 8 and 9). Aging intensified carbonyl (C=O, ~1700 cm^{-1}) and sulfoxide (S=O, ~1030 cm^{-1}) absorbances, correlating with SARA-observed aromatic depletion (49.5% → 35.9%) [39]. Bio-oil incorporation produced systematic, dosage-dependent intensification of aliphatic C–H stretching modes (2920 cm^{-1}, 2850 cm^{-1})—a chemical fingerprint for maltene-phase restoration [40]. Quantitative peak area analysis revealed that 20% SBO increased aliphatic absorbance by 78% relative to aged binder, compared to 43% for equivalent RSO treatment.

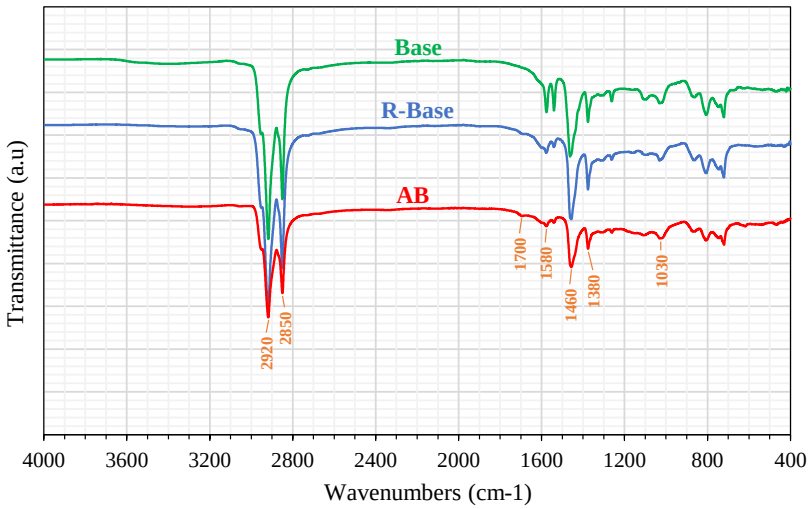

Figure 8. The FTIR Spectral Analysis of Asphalt Base Binder

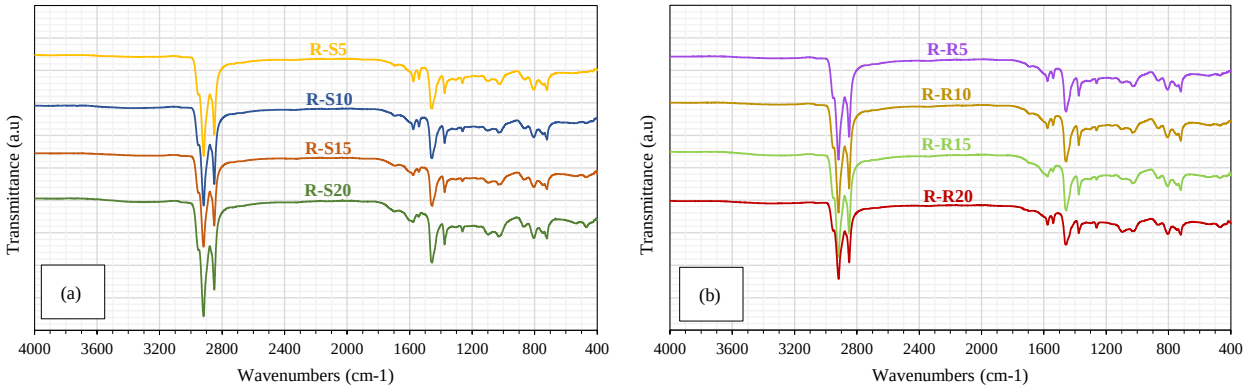

Figure 9. The Spectra Analysis of FTIR: a) SBO-rejuvenated Binders; b) RSO-rejuvenated Binders

The persistence of carbonyl and sulfoxide peaks in rejuvenated binders requires careful interpretation. These features likely reflect contributions from the inherent oxygenated character of bio-oils in addition to residual aging-related oxidation. Bio-oils contain mobile ketones and esters attached to flexible aliphatic chains, whereas aged asphalt harbors rigid carbonyls in condensed polyaromatic networks. This distinction is mechanistically significant, as bio-oil's mobile polar groups function as molecular lubricants rather than stiffening agents [38].

3.6. Viscoelastic Response Under Cyclic Loading: MSCR Behavior

MSCR testing at 0.1 kPa and 3.2 kPa simulates light and heavy traffic loading, respectively. Strain evolution revealed remarkable homogenization across formulations (Figures 10 and 11). At 0.1 kPa and 70°C, all rejuvenated binders exhibited comparable strain (~1,200–1,500%) regardless of bio-oil type or dosage—a finding unpredictable from SARA analysis. This uniformity contrasts with the 119% penetration differential and near-identical Ic values (0.541–0.572), confirming that bulk chemical indices provide no predictive capacity for viscoelastic recovery after aging.

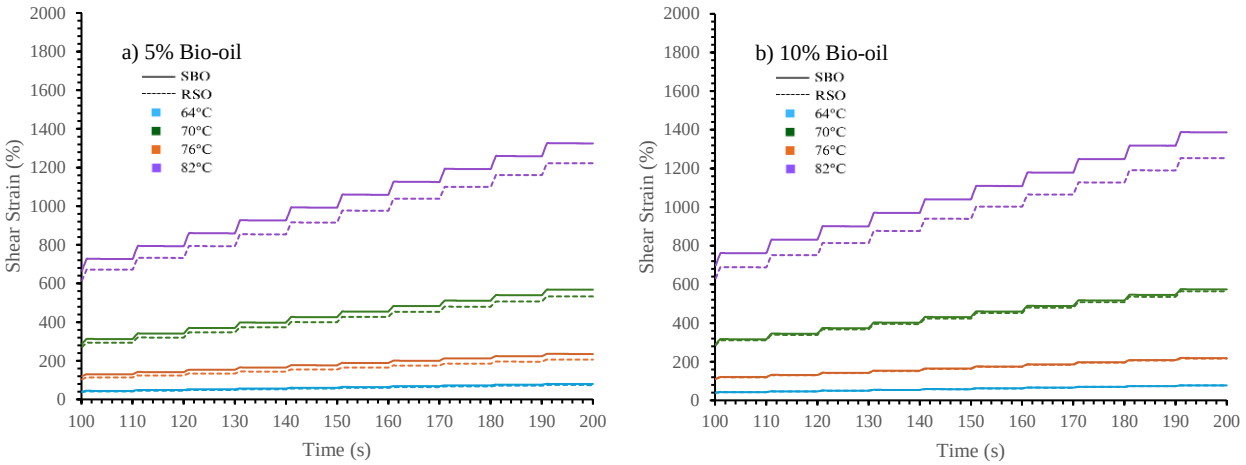

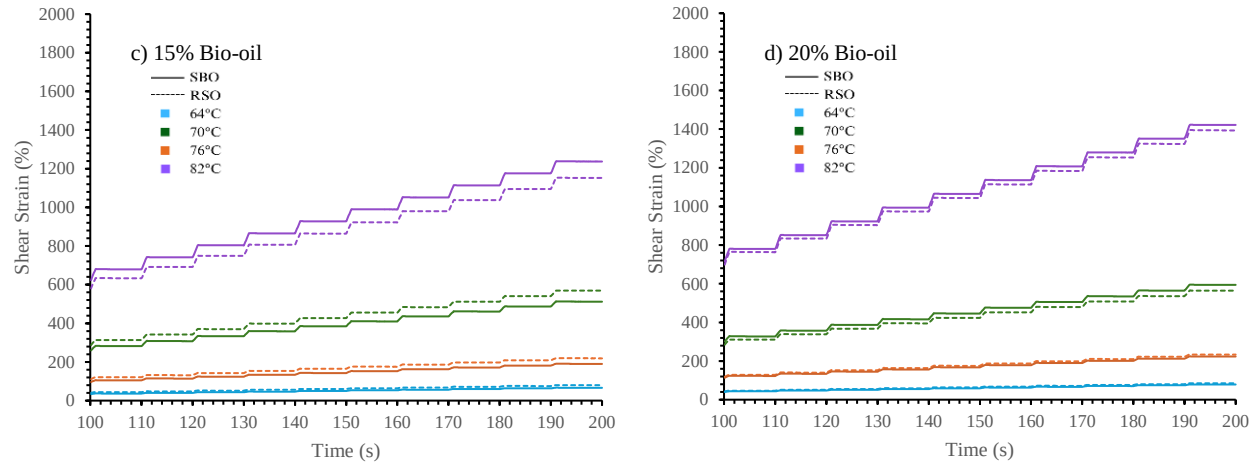

Figure 10. Shear Strain Curves of Rejuvenated Asphalt Binders @ 0.1 kPa

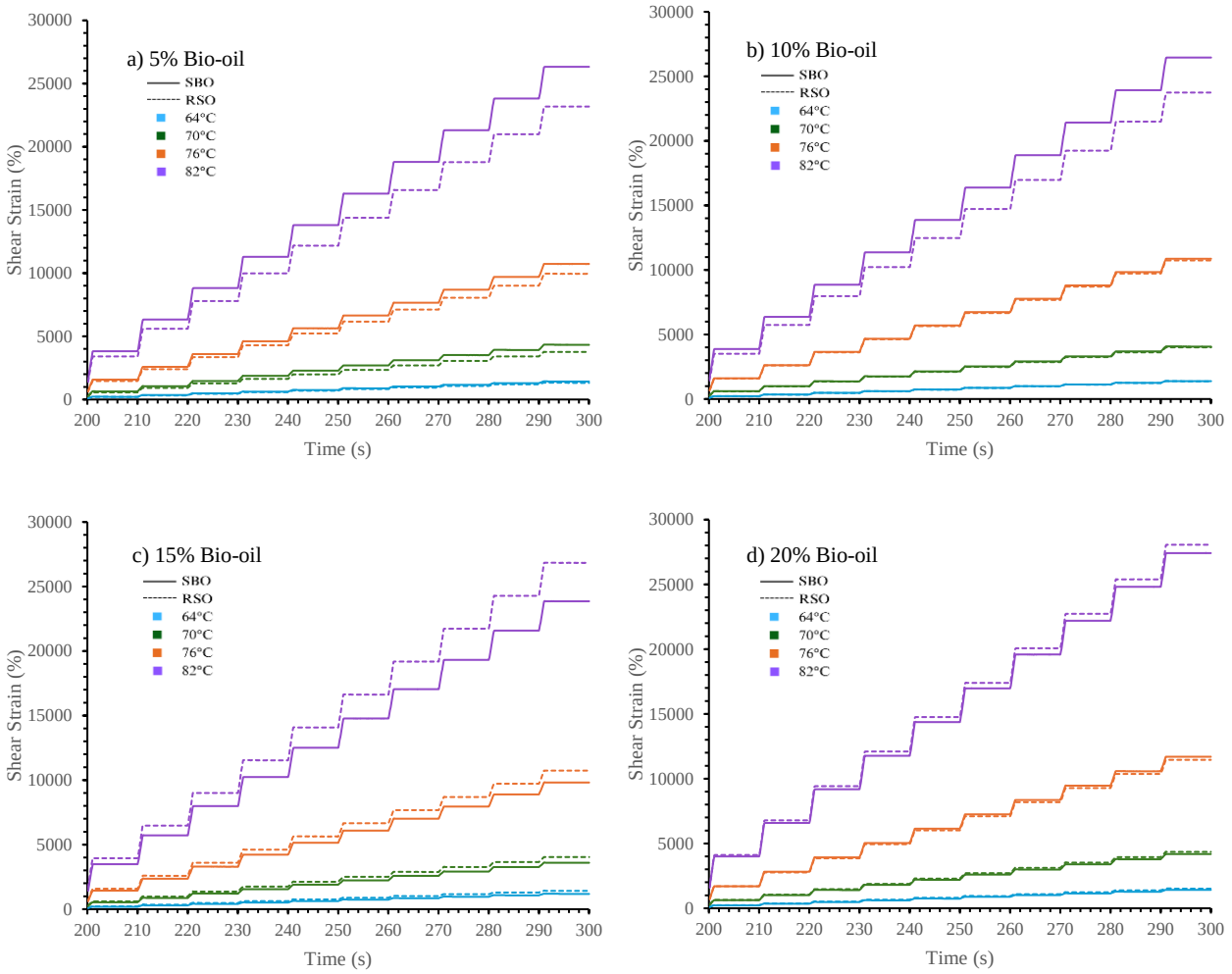

Figure 11. Shear Strain Curves of Rejuvenated Asphalt Binders @ 3.2 kPa

The thermal instability of low-molecular-weight bio-oil components provides the mechanistic basis. Compounds with boiling points below 180°C—constituting approximately 35–40% of bio-oil mass—volatilize during RTFO conditioning, partially reversing rejuvenation. This mechanism is corroborated by findings from the companion study [12], which demonstrated a dosage-dependent durability paradox: formulations with the best fresh performance (15–20%) exhibited the weakest post-aging durability, while the lowest dosage (5% SBO) provided the strongest aging mitigation. The present MSCR convergence is consistent with this pattern, as volatile loss homogenizes the remaining binder microstructure regardless of initial dosage (Figure 12).

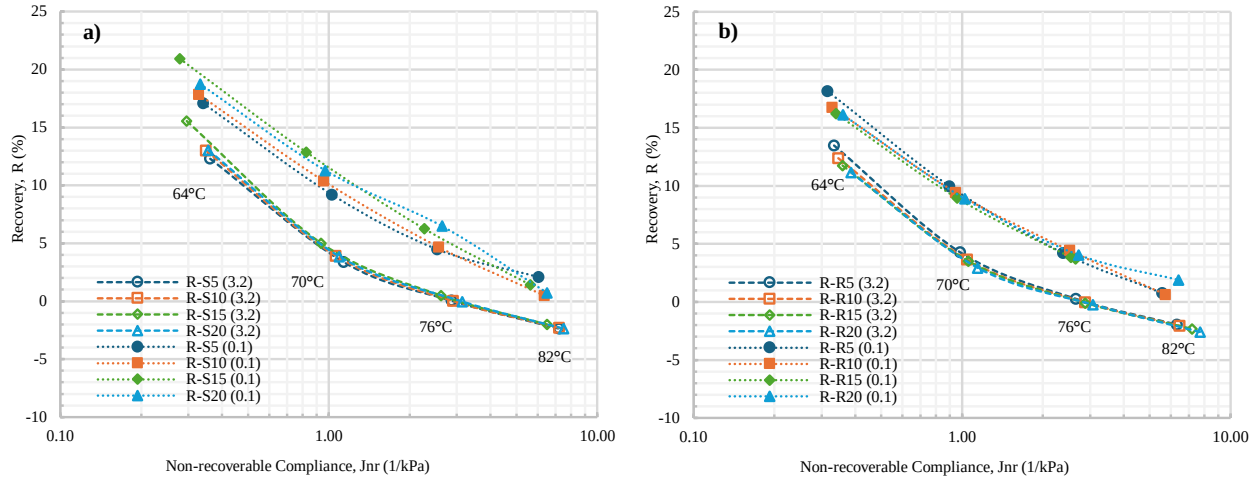

Figure 12. The MSCR Curves of Asphalt Binders: a) SBO-rejuvenated; b) RSO-rejuvenated

Despite strain homogenization, recovery parameters revealed nuanced behavior. At 3.2 kPa and 70°C, R-S15 (15% SBO) achieved %R of 18.4% with Jnr of 0.89 kPa^{-1}, outperforming all formulations. This dosage represents an optimum balancing softening capacity against thermal stability. R-R5 (5% RSO) was optimal within the RSO group (%R: 14.2%; Jnr: 1.12 kPa^{-1}), suggesting higher RSO dosages contribute excess incompatible components. These values are comparable to published data for waste cooking oil rejuvenated binders (10–20% recovery) [15, 29] and fall within the range for polymer-modified binders [14]. Temperature sensitivity dominated: %R collapsed from ~25% to <5% and Jnr escalated exponentially from 64°C to 82°C. At 82°C, all binders exceeded the Jnr threshold of 4.5 kPa^{-1}, representing rheological failure [15].

The optimal dosage of 15% SBO identified through MSCR aligns with the dosage optimization reported by Hu et al. [44], who proposed a rejuvenation index framework suggesting 12–18% as the effective range for bio-oil rejuvenators. However, the present study reveals a critical nuance absent from that framework: the MSCR-optimal dosage (15% SBO) differs from the penetration-optimal dosage (20% SBO), demonstrating that different performance metrics yield different optimal formulations. This finding reinforces the central argument that no single chemical or physical indicator can serve as a universal optimization criterion for rejuvenated binders. El-Sherbeni et al. [45] similarly reported that biomass-derived bio-oils at 10–15% provided the best balance between stiffness reduction and recovery retention, consistent with the present results.

3.7. Comparative Rutting Resistance: Rejuvenated vs. Virgin Binder

Rejuvenated binders demonstrated superior rutting resistance but inferior elastic recovery relative to virgin material (Figure 13). At 70°C and 3.2 kPa, rejuvenated binders achieved Jnr of 0.89–1.42 kPa^{-1} versus 2.31 kPa^{-1} for the base binder—a 38–61% improvement. This enhancement stems from irreversible aging-induced molecular associations that persist after bio-oil treatment, increasing molecular weight and entanglement density.

However, rejuvenated binders recovered only 12–18% of imposed strain versus 23% for neat binder, indicating bio-oils restore fluidity without fully regenerating molecular mobility. This dichotomy underscores the decoupling between chemical and mechanical restoration: bulk compositional recovery cannot account for irreversible aging-induced molecular associations that govern cyclic recovery [15, 45].

The recovery deficit observed in rejuvenated binders (12–18% vs. 23% for virgin) is consistent with findings from multiple independent studies. Liu et al. [15] reviewed MSCR data across various modified binder systems and reported that rejuvenated RAP binders typically recover 40–70% less strain than virgin binders at equivalent Jnr values, confirming that aging-induced structural damage is only partially reversible. Prosperi & Bocci [43] attributed this persistent recovery deficit to irreversible condensation reactions forming C–C and ether crosslinks within the asphaltene fraction that cannot be reversed by solvent-based rejuvenation. The present data are fully consistent with these mechanisms and extend the observation specifically to agricultural bio-oil systems, where the combination of volatile loss and persistent crosslinking creates the decoupling between chemical restoration (SARA normalization) and mechanical recovery (MSCR %R deficit).

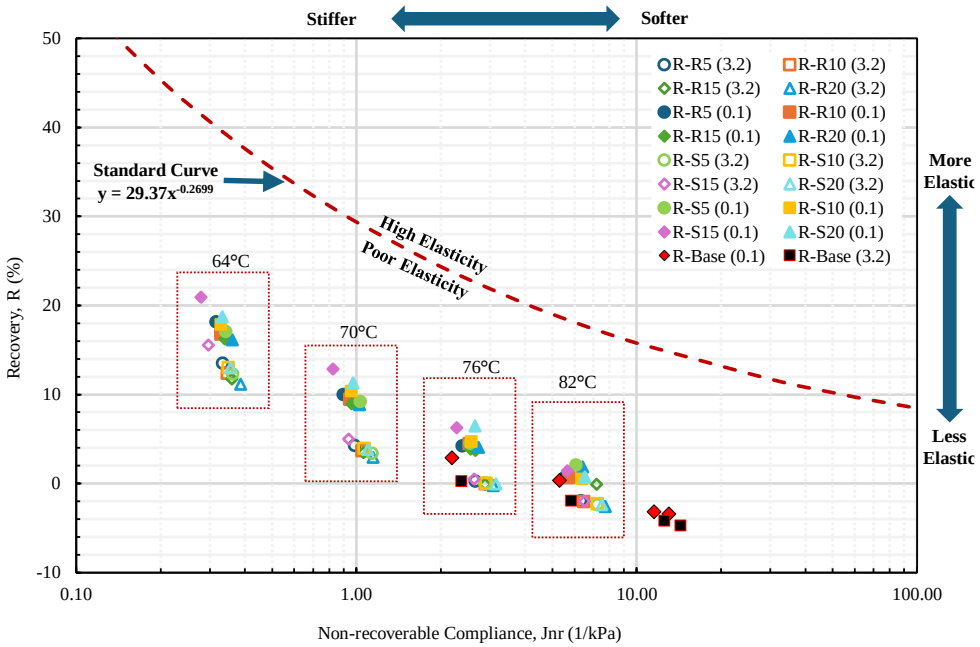

Figure 13. The MSCR Curve Comparison of Rejuvenated and Base Binders

3.8. Traffic Load Classification

An Equivalent Single Axle Load (ESAL) classification according to AASHTO M 332 translates laboratory rheological data into practical pavement performance predictions (Table 5).

Table 5. ESAL Classification

Sample	Temperature			
	64°C	70°C	76°C	82°C
R-S5	E	H	S	Failed
R-S10	E	H	S	Failed
R-S15	E	H	S	Failed
R-S20	E	H	S	Failed
R-R5	E	H	S	Failed
R-R10	E	H	S	Failed
R-R15	E	H	S	Failed
R-R20	E	H	S	Failed
R-Base	S	Failed	Failed	Failed

All rejuvenated binders achieved identical ESAL grading trajectories regardless of bio-oil type or dosage, confirming that neither physical property tests nor bulk chemical indices could have predicted this converged MSCR performance. The neat base binder achieved only 'S' grade at 64°C, confirming that rejuvenated RAP binders outperform unaged neat material for high-temperature applications. This is consistent with previous studies [14, 45] attributing the effect to residual asphaltene enrichment and persistent crosslinking.

4. Conclusion

This study characterized the decoupling between bulk chemical composition and high-temperature viscoelastic recovery in asphalt binders rejuvenated with SBO and RSO pyrolytic bio-oils. The results confirm that chemical restoration and mechanical recovery operate through fundamentally independent mechanisms.

Although both bio-oils restored SARA fractions to nearly identical levels (Ic = 0.541–0.572), their mechanical responses differed substantially prior to aging. SBO at 20% restored penetration to 79 dmm—exceeding the virgin binder—while RSO achieved only 36 dmm, a 119% differential. Softening point and viscosity corroborated these differences, attributable to SBO's aromatic-rich composition (63% aromatic solvent fraction). These physical property differences were not reflected in the SARA-derived colloidal instability indices, which converged across all formulations.

Following RTFO aging, MSCR responses converged across all formulations, yielding identical ESAL grading trajectories (E–H–S–Fail from 64–82°C) regardless of pre-aging differences. This convergence is attributed to selective volatilization of low-molecular-weight bio-oil components, consistent with the dosage paradox identified in the companion study [12]. Additionally, irreversible aging-induced molecular associations persist after treatment, constraining elastic recovery (12–18% vs. 23% for neat binder) while enhancing rutting resistance (38–61% Jnr improvement).

Chemical indices remain useful for assessing compositional changes but should not serve as sole predictors of rutting performance. Performance-based rheological testing—particularly MSCR—is essential for reliable evaluation. Together with the companion study's LAS fatigue findings [12], these results establish that both high-temperature and intermediate-temperature performance assessments are necessary to comprehensively evaluate bio-oil rejuvenated systems. Future research should incorporate mixture-level validation, investigate volatile retention strategies, explore hybrid formulations combining bio-oils with synthetic antioxidants and polymer modifiers [12], and employ complementary molecular techniques (GPC, NMR) to better understand structure–property relationships in rejuvenated systems.

5. Declarations

5.1. Author Contributions

Conceptualization, M.H. and P.C.; methodology, M.H., S.C., and P.C.; investigation, M.H.; resources, M.H.; validation, M.H. and P.C.; visualization, M.H.; writing—original draft preparation, M.H.; writing—review and editing, P.C.; supervision, P.C. All authors have read and agreed to the published version of the manuscript.

5.2. Data Availability Statement

The data presented in this study are available on request from the corresponding author.

5.3. Funding and Acknowledgments

This work was supported by King Mongkut's Institute of Technology Ladkrabang Research Fund under the KMITL Doctoral Scholarship [KDS2021/020].

5.4. Conflicts of Interest

The authors declare no conflict of interest.

6. References

[1] Yang, T., He, Z., Huang, G., Zhao, Y., Fu, J., Xiang, H., & Zhou, Y. (2023). Study on materials composition and process parameters of polyurethane-modified asphalt synthesized in-situ by the one-shot process. Construction and Building Materials, 374. doi:10.1016/j.conbuildmat.2023.130661.

[2] Li, J., Xing, X., Hou, X., Wang, T., Wang, J., & Xiao, F. (2022). Determination of SARA fractions in asphalts by mid-infrared spectroscopy and multivariate calibration. Measurement: Journal of the International Measurement Confederation, 198. doi:10.1016/j.measurement.2022.111361.

[3] Luo, H., Huang, X., Tian, R., Huang, J., Zheng, B., Wang, D., & Liu, B. (2021). Analysis of relationship between component changes and performance degradation of Waste-Oil-Rejuvenated asphalt. Construction and Building Materials, 297. doi:10.1016/j.conbuildmat.2021.123777.

[4] Zahoor, M., Nizamuddin, S., Madapusi, S., & Giustozzi, F. (2021). Recycling asphalt using waste bio-oil: A review of the production processes, properties and future perspectives. Process Safety and Environmental Protection, 147, 1135–1159. doi:10.1016/j.psep.2021.01.032.

[5] Liu, F., Zhang, X., Zhou, Z., Cao, J., & Wang, X. (2023). A novel approach to predict the rheological properties of rejuvenated binder subject to secondary aging. Construction and Building Materials, 389. doi:10.1016/j.conbuildmat.2023.131788.

[6] Kumar, V., & Aggarwal, P. (2025). Application of Natural and Waste Oils as Rejuvenator in Reclaimed Asphalt Pavement: A Review. International Journal of Pavement Research and Technology, 18(4), 805–828. doi:10.1007/s42947-023-00388-7.

[7] Cavalli, M. C., Wu, W., & Poulikakos, L. (2024). Bio-based rejuvenators in asphalt pavements: A comprehensive review and analytical study. Journal of Road Engineering, 4(3), 282–291. doi:10.1016/j.jreng.2024.04.007.

[8] Zhang, Y., Si, C., Fan, T., Zhu, Y., Li, S., Ren, S., & Lin, P. (2023). Research on the optimal dosage of Bio-Oil/Lignin composite modified asphalt based on rheological and Anti-Aging properties. Construction and Building Materials, 389. doi:10.1016/j.conbuildmat.2023.131796.

[9] de Medeiros Melo Neto, O., de Figueiredo Lopes Lucena, L. C., Silva, I. M., de Figueiredo Lopes Lucena, L., Mendonça, A. M. G. D., da Silva Lopes, A. M., da Silva, F. M. M., de Amorim, A. G., & de Oliveira Neto, H. R. (2023). Effects of the addition of fatty acid from soybean oil sludge in recycled asphalt mixtures. Environmental Science and Pollution Research, 30(17), 50174–50197. doi:10.1007/s11356-023-25808-w.

[10] Park, K. B., Kim, J. S., Pahlavan, F., & Fini, E. H. (2022). Biomass Waste to Produce Phenolic Compounds as Antiaging Additives for Asphalt. ACS Sustainable Chemistry and Engineering, 10(12), 3892–3908. doi:10.1021/acssuschemeng.1c07870.

[11] Liu, S., Wang, H., & Yang, J. (2025). Utilization of biomass waste to produce phenol-rich bio-oil for enhancing the long-term aging resistance of rejuvenated bitumen. Materials and Structures/Materiaux et Constructions, 58(3), 94. doi:10.1617/s11527-025-02620-1.

[12] Hutabarat, M., Chamwon, S., & Chaturabong, P. (2026). Advanced characterization of bio-rejuvenated asphalt systems using agricultural waste pyrolytic oils: Integrated assessment of chemical composition, rheological, and aging performance. Construction and Building Materials, 518, 145801. doi:10.1016/j.conbuildmat.2026.145801.

[13] Xu, Y., Zhang, E., & Shan, L. (2019). Effect of SARA on rheological properties of asphalt binders. Journal of Materials in Civil Engineering, 31(6), 04019086. doi:10.1061/(asce)mt.1943-5533.0002723.

[14] Zeng, G., Zhang, J., Huang, H., Xiao, X., & Yan, C. (2023). A Comparative Study for Creep and Recovery Behavior Characterization of Modified Bitumens Using the MSCR Test. Coatings, 13(8), 1445. doi:10.3390/coatings13081445.

[15] Liu, H., Zeiada, W., Al-Khateeb, G. G., Shanableh, A., & Samarai, M. (2021). Use of the multiple stress creep recovery (MSCR) test to characterize the rutting potential of asphalt binders: A literature review. Construction and Building Materials, 269. doi:10.1016/j.conbuildmat.2020.121320.

[16] de Oliveira, Y. M. M., Cittadella, P. T., Rohde, L., & Thives, L. P. (2023). Simulation of the Time Needed for Long-Term Asphalt Ageing in the Rolling Thin Film Oven Relative to That of the Pressure Ageing Vessel. Materials, 16(22), 7081. doi:10.3390/ma16227081.

[17] Wang, T., Jiang, W., Xiao, J., Guo, D., Yuan, D., Wu, W., & Wang, W. (2022). Study on the blending behavior of asphalt binder in mixing process of hot recycling. Case Studies in Construction Materials, 17. doi:10.1016/j.cscm.2022.e01477.

[18] Tawkaew, S., Unsomsri, N., Asadamongkon, P., Jansri, S. N., Wiriyasart, S., & Kaewluan, S. (2025). Distillation study of light bio-oil from palm fresh fruit pyrolysis for enhanced bio-gasoline characteristics through blending with gasohol E85. Energy Nexus, 18. doi:10.1016/j.nexus.2025.100432.

[19] Kumar, M., Upadhyay, S. N., & Mishra, P. K. (2022). Pyrolysis of Sugarcane (Saccharum officinarum L.) Leaves and Characterization of Products. ACS Omega, 7(32), 28052–28064. doi:10.1021/acsomega.2c02076.

[20] Zhou, J., Dong, Z., Cao, L., Li, L., Yu, Y., Sun, Z., Zhou, T., & Chen, Z. (2024). Rheological evaluation of paving asphalt binder containing bio-oil from rice straw pyrolysis. Case Studies in Construction Materials, 20. doi:10.1016/j.cscm.2024.e03202.

[21] Toscano Miranda, N., Lopes Motta, I., Maciel Filho, R., & Wolf Maciel, M. R. (2021). Sugarcane bagasse pyrolysis: A review of operating conditions and products properties. Renewable and Sustainable Energy Reviews, 149. doi:10.1016/j.rser.2021.111394.

[22] Uddin, I., Sohail, M., Hussain, M. I., Alhokbany, N., Amaro-Gahete, J., & Estévez, R. (2023). Probing the Pyrolysis Process of Rice Straw over a "Dual-Catalyst Bed" for the Production of Fuel Gases and Value-Added Chemicals. Sustainability (Switzerland), 15(14), 11057. doi:10.3390/su151411057.

[23] Alfe, M., Gargiulo, V., Ruoppolo, G., Cammarota, F., Calandra, P., Oliviero Rossi, C., Loise, V., Porto, M., Di Capua, R., & Caputo, P. (2024). Microstructural modifications in bitumens rejuvenated by oil from pyrolysis of waste tires. Frontiers in Chemistry, 12, 1512905. doi:10.3389/fchem.2024.1512905.

[24] Bouchonnet, S. (2013). Introduction to GC–MS coupling. CRC Press (Taylor & Francis Group), Boca Raton, United States.

[25] Yan, S., Dong, Q., Chen, X., Zhou, C., Dong, S., & Gu, X. (2022). Application of waste oil in asphalt rejuvenation and modification: A comprehensive review. Construction and Building Materials, 340. doi:10.1016/j.conbuildmat.2022.127784.

[26] Chen, C., Lu, J., Ma, T., Zhang, Y., Gu, L., & Chen, X. (2023). Applications of vegetable oils and their derivatives as Bio-Additives for use in asphalt binders: A review. Construction and Building Materials, 383. doi:10.1016/j.conbuildmat.2023.131312.

[27] Wetekam, J., & Mollenhauer, K. (2024). FTIR spectroscopy analysis assessment of reclaimed asphalt at asphalt mixing plants to optimize the recycling. Transportation Engineering, 16. doi:10.1016/j.treng.2024.100242.

[28] Zhang, D., Chen, M., Wu, S., Liu, J., & Amirkhanian, S. (2017). Analysis of the relationships between waste cooking oil qualities and rejuvenated asphalt properties. Materials, 10(5), 508. doi:10.3390/ma10050508.

[29] Zhou, X., Moghaddam, T. B., Chen, M., Wu, S., Zhang, Y., Zhang, X., Adhikari, S., & Zhang, X. (2021). Effects of pyrolysis parameters on physicochemical properties of biochar and bio-oil and application in asphalt. Science of the Total Environment, 780, 146448. doi:10.1016/j.scitotenv.2021.146448.

[30] Kunanusont, N., Sangpetngam, B., & Somwangthanaroj, A. (2021). Asphalt incorporation with ethylene vinyl acetate (Eva) copolymer and natural rubber (nr) thermoplastic vulcanizates (tpvs): Effects of tpv gel content on physical and rheological properties. Polymers, 13(9), 1397. doi:10.3390/polym13091397.

[31] Pahlavan, F., Lamanna, A., Park, K. B., Kabir, S. F., Kim, J. S., & Fini, E. H. (2022). Phenol-rich bio-oils as free-radical scavengers to hinder oxidative aging in asphalt binder. Resources, Conservation and Recycling, 187. doi:10.1016/j.resconrec.2022.106601.

[32] Wang, Y., Wang, W., & Wang, L. (2022). Understanding the relationships between rheology and chemistry of asphalt binders: A review. Construction and Building Materials, 329. doi:10.1016/j.conbuildmat.2022.127161.

[33] Liu, J., Lv, S., Peng, X., & Yang, S. (2021). Improvements on performance of bio-asphalt modified by castor oil-based polyurethane: An efficient approach for bio-oil utilization. Construction and Building Materials, 305. doi:10.1016/j.conbuildmat.2021.124784.

[34] Li, C., Rajib, A., Sarker, M., Liu, R., Fini, E. H., & Cai, J. (2021). Balancing the Aromatic and Ketone Content of Bio-oils as Rejuvenators to Enhance Their Efficacy in Restoring Properties of Aged Bitumen. ACS Sustainable Chemistry and Engineering, 9(20), 6912–6922. doi:10.1021/acssuschemeng.0c09131.

[35] Fardhyanti, D. S., Megawati, Chafidz, A., Prasetiawan, H., Raharjo, P. T., Habibah, U., & Abasaeed, A. E. (2024). Production of bio-oil from sugarcane bagasse by fast pyrolysis and removal of phenolic compounds. Biomass Conversion and Biorefinery, 14(1), 217–227. doi:10.1007/s13399-022-02527-9.

[36] Joni, H. H., Al-Rubaee, R. H. A., & Al-zerkani, M. A. (2019). Rejuvenation of aged asphalt binder extracted from reclaimed asphalt pavement using waste vegetable and engine oils. Case Studies in Construction Materials, 11. doi:10.1016/j.cscm.2019.e00279.

[37] Zargar, M., Ahmadinia, E., Asli, H., & Karim, M. R. (2012). Investigation of the possibility of using waste cooking oil as a rejuvenating agent for aged bitumen. Journal of Hazardous Materials, 233, 254-258. doi:10.1016/j.jhazmat.2012.06.021.

[38] Wang, J., Xu, S., Zhu, S., Tian, Q., Yang, X., Pipintakos, G., Ren, S., & Wu, S. (2024). The Rejuvenation Effect of Bio-Oils on Long-Term Aged Asphalt. Materials, 17(13), 3316. doi:10.3390/ma17133316.

[39] Furtana Yalcin, B., & Yilmaz, M. (2024). Investigation of the Performance of Bio-Oils from Three Different Agricultural Wastes as Rejuvenators for Recycled Asphalt. Turkish Journal of Civil Engineering, 35(3), 95–123. doi:10.18400/tjce.1320185.

[40] Zhang, R., You, Z., Wang, H., Ye, M., Yap, Y. K., & Si, C. (2019). The impact of bio-oil as rejuvenator for aged asphalt binder. Construction and Building Materials, 196, 134–143. doi:10.1016/j.conbuildmat.2018.10.168.

[41] Zhang, M., Hao, P., Dong, S., Li, Y., & Yuan, G. (2020). Asphalt binder micro-characterization and testing approaches: A review. Measurement: Journal of the International Measurement Confederation, 151. doi:10.1016/j.measurement.2019.107255.

[42] Wang, T., Wang, J., Hou, X., & Xiao, F. (2021). Effects of SARA fractions on low temperature properties of asphalt binders. Road Materials and Pavement Design, 22(3), 539–556. doi:10.1080/14680629.2019.1628803.

[43] Prosperi, E., & Bocci, E. (2021). A review on bitumen aging and rejuvenation chemistry: Processes, materials and analyses. Sustainability (Switzerland), 13(12), 6523. doi:10.3390/su13126523.

[44] Hu, Y., Ryan, J., Sreeram, A., Allanson, M., Pasandín, A. R., Zhou, L., Singh, B., Wang, H., & Airey, G. D. (2024). Optimising the dosage of bio-rejuvenators in asphalt recycling: A rejuvenation index-based approach. Construction and Building Materials, 433. doi:10.1016/j.conbuildmat.2024.136761.

[45] El-Sherbeni, A. A., Awed, A. M., Gabr, A. R., & El-Badawy, S. M. (2025). Biomass-Derived Bio-Oil for asphalt binder applications: production feasibility and performance enhancement. Construction Materials, 5(1), 11. doi:10.3390/constrmater5010011.